ALEPH 94-128
PHYSIC 94-112
P. Bourdon
20.07.1994

Measurement of ρ meson production rates in the $\tau \rightarrow 3\pi\pi^0$channel

Pierre BOURDON

LPNHE Ecole Polytechnique, IN2P3-CNRS

Using Aleph data until 1992, the decay of the τ into three charged π and one π^0 is shown to be accountable in terms of an incoherent sum of 2 processes: one proceeding through an intermediate $\omega - \pi$, the other through an intermediate $\rho - \pi - \pi$ system. The contribution from a possible p-wave $(\rho - \rho)$ system is much lower than the latter and unobservable. The $\rho - \pi - \pi$ decay is built out of three components corresponding to the three possible charges of the ρ. Their respective contributions have been fitted with reference distributions obtained from the theoretical model used in TAUOLA. The result, obtained by neglecting the small interference terms between the three components and constraining to unit sum, is:

$$\begin{cases} \tau^{\pm} \rightarrow \rho^{unl}\pi^{lik}\pi^{lik} & : \; 43.8 \pm 3.1_{stat} \pm 3.9_{syst} \quad \% \\ \tau^{\pm} \rightarrow \rho^{lik}\pi^{unl}\pi^{lik} & : \; 34.8 \pm 3.4_{stat} \pm 3.0_{syst} \quad \% \\ \tau^{\pm} \rightarrow \rho^{0}\ \pi^{lik}\pi^{0} & : \; 21.4 \pm 3.4_{stat} \pm 3.0_{syst} \quad \% \end{cases}$$

1 Theoretical Overview

The exact structure of the current for the decay of the τ into 4π is still unknown. We have already shown [2] that there is production of an intermediate $\omega\pi$ system at the level of 51%. This process does not strongly interfere with the one of interest in this paper because of the narrowness of the ω resonance.
The remaining 49% of the decays must also consist of 4π systems in a $J^P = 1^-$ state (in the isospin conservation limit) which implies one, three or more p-waves. Because of the limited available phase space, the favoured solution is to have one relative orbital p-wave between two pions, i.e. one ρ meson. The next possibility is to have three p-waves which corresponds to the $(\rho-\rho)_p$ decay. One sees that this is strongly suppressed when compared to the $\rho-\pi-\pi$ decay.
In this analysis, we make use of the model presented in [1] which is the one implemented in TAUOLA. We must make it clear that it has only been used as a basis for refitting its parameters since it implies relations between the different ρ production rates that are in strong disagreement with this analysis.
This model basically starts from a low energy chirally symmetric lagrangian generating effective 2,3 and 4 pion vertices. The authors obtain the following current for the process $\tau^{\pm} \rightarrow \pi_1^{lik}\pi_2^{lik}\pi^{unl}\pi^0$:

$$J_\mu = \frac{2\sqrt{3}}{f_\pi^2}[2(q_{unl}-q_0)^\nu A_{\mu\nu}^{unl\ 0} + (q_{lik\ 1}-q_{unl})^\nu A_{\mu\nu}^{1\ unl} + (q_{lik\ 2}-q_{unl})^\nu A_{\mu\nu}^{2\ unl}]$$

where the tensor structure is given by:

$$A_{\mu\nu}^{ik} = g_{\mu\nu} - \sum_{l\neq i,k} \frac{(Q-2q_l)_\mu (Q-q_l)_\nu}{(Q-q_l)^2}$$

(Q is the sum of the four momenta)
One sees a sum of three independently conserved terms (in the limit of massless pions) with non-trivial Lorenz structure. Now this current must account for the final state interaction which we said mainly consists in the formation of a ρ resonance (the other 2 pions are taken to be non-interacting). The way to introduce it in this current is of course to multiply each term by a Breit-Wigner like form-factor which will describe the resonances in the $m_{\pi\pi}$ mass spectra.
The extrapolated current reads:

$$J'_\mu = \frac{2\sqrt{3}}{f_\pi^2}[2(q_{unl}-q_0)^\nu A_{\mu\nu}^{unl\ 0} F(s_{unl\ 0}) + (q_{lik\ 1}-q_{unl})^\nu A_{\mu\nu}^{1\ unl} F(s_{1\ unl}) + (q_{lik\ 2}-q_{unl})^\nu A_{\mu\nu}^{2\ unl} F(s_{2\ unl})]$$

where the form factors are:

$$F(s) = \frac{m_\rho^2 - i m_\rho \Gamma_\rho}{m_\rho^2 - s - i m_\rho \Gamma_\rho}$$

One immediately notices the absence of resonance in the like-charge channel which is a striking feature of that model. Furthermore, since we want to retrieve the initial current in the low energy limit, the form factors must satisfy $F(0)=1$ which 0 them to produce

twice as much unlike-charged rhos as neutral rhos.
Finally, this particular current neglects both the interactions of the 2 pions in the s-wave state and that of the rho with an outside pion which would resonate in an a1(1260) (in a relative s-wave). In this limit, their scheme also predicts that the $\rho\pi\pi$ with one π^0 rate is twice that of $\rho^\pm\pi^0\pi^0$ (at any Q^2 in fact). One could also test this prediction by studying the experimentally more delicate $\tau^\pm \longrightarrow \pi^\pm 3\pi^0$ decay which, again insofar as the other final state interactions can be neglected or subtracted, should be twice lower than the branching ratio $\tau^\pm \longrightarrow \rho\pi\pi$ measured in this work.

On the experimental side, ARGUS [3] has presented an analysis based on a statistic roughly three times lower than the present one (which is about 50K τ pairs) and found:

$$\begin{cases} \tau^\pm \longrightarrow \rho^{unl}\pi^{lik}\pi^{lik} & : \ 15.6 \pm 4.7 \pm 0.6\% \\ \tau^\pm \longrightarrow \rho^{lik}\pi^{unl}\pi^{lik} & : \ 40.6 \pm 7.8 \pm 1.6\% \\ \tau^\pm \longrightarrow \rho^0\ \pi^{lik}\pi^0 & : \ 46.9 \pm 6.3 \pm 3.1\% \end{cases}$$

I have translated their result given in terms of fractions relative to the whole $3\pi\pi^0$ decay the same way I did with mine. This means that I divide it by the proportion of the $3\pi\pi^0$ decay estimated to proceed from a $\rho\pi\pi$ intermediate. The sum of these 3 figures is in my case constrained to unity while this is not the case for [3] which might indicate that this manipulation of their result is not rigourously correct.

2 Event selection and ω suppression

2.1 Selection of the $3\pi\pi^0$ candidates

We use the selection described in [2] from which we have already derived:

$$BR(\tau \longrightarrow 3\pi\pi^0) = 4.25 \pm .13_{stat} \pm .13_{syst}\%$$

and [1]:

$$\frac{\Gamma(\tau \longrightarrow \omega\pi) \times Br(\omega \longrightarrow \pi^+\pi^-\pi^0)}{\Gamma(\tau \longrightarrow 3\pi\pi^0)} = 45.0 \pm 1.9^{+2.5}_{-2.6}\%$$

We are insensitive to $BR(\tau \longrightarrow 3\pi\pi^0)$ in this analysis but shall use as an input the proportion $\alpha \equiv \frac{\Gamma(\tau\rightarrow\omega\pi)}{\Gamma(\tau\rightarrow 3\pi\pi^0)}$. From [2] and $Br(\omega \longrightarrow \pi^+\pi^-\pi^0) = 88.8\%$ we get:

$$\alpha = 50.7\%$$

2.2 Suppression of the $\omega\pi$ events:

In our selected sample, we have [2] a background from τ events of 13% and from non-τ of less than 1%. More important is that half of the remaining events are from $\tau \longrightarrow \omega\pi$. It is necessary to reduce this figure before attempting any meaningful fit for the various ρ rates. Fortunately, the ω resonance is narrow enough to simply cut it out i.e. to reject all events with $m_{(\pi^{unl}\pi_1^{lik}\pi^0)}$ or $m_{(\pi^{unl}\pi_2^{lik}\pi^0)}$ between 700 and 870 MeV. This rejection gets

[1] This value has slightly changed since [2] following a reevaluation of the efficiency ratio used to deduce it from the raw (fit) value

rid of 93% of the $\omega\pi$ decays while preserving around 78% of the $\rho\pi\pi$ (figure 1) and alters the background level but we shall return in greater detail to this question in subsection 3.3.
We show on figure 2 the 4-pions invariant mass for the data and the Monte-Carlo after this cut. The aim is to demonstrate their general agreement. Otherwise, since we have ρ peaks already distorted by phase-space limitation, we might have Monte-Carlo spectra very different from those of the data (in particular, shifted ρ peaks). We see here and on the fits that this is not the case.

3 Monte-Carlo samples

3.1 Description of the samples

We have produced for this analysis 3 Monte-Carlo samples which will be used in addition to the one already elaborated for the $\omega\pi$ study [2]. They will be used to estimate the selection acceptance and more important the ω suppression cut efficiencies for the various subprocesses.

- The pure $\tau^{\pm} \rightarrow \omega\pi^{\pm}$ events are necessary to estimate the proportion that survives their suppression cut. This remaining population will later be subtracted in the fit to make it more accurate. As explained in [2], their dynamics is well established and they do not practically interfere with the $\rho\pi\pi$ current of interest here so that their impact on our precision is eventually limited and under control.
- The 3 "$\rho\pi\pi$" subprocesses simulated are:
  1. First the $\tau^{\pm} \rightarrow \rho^{unl}\pi^{lik}\pi^{lik}$ process alone which is further necessary to obtain reference distributions for the fit as explained in subsection 4.1.
  2. Next is the $\tau^{\pm} \rightarrow \rho^{0}\ \pi^{lik}\pi^{0}$ process alone which checks and complements the afore mentioned reference distributions. It also shows us that the ρ^{unl} and ρ^{0} peaks are similar despite the fact that the first uses a refitted π^{0} (from QPI0DO) and the latter 2 charged tracks. We see on figure 3 that the reference distributions are indistinguishable which allows us to retain the same 3 for any of the 3 possible $\rho\pi\pi$.
  3. Last is the standard (in KORL06) $\rho\pi\pi$ part of the $\tau^{\pm} \rightarrow 3\pi\pi^{0}$ current which shall allow us to test the effect of the interferences between its components (standard $= \ 2/3 \times \rho^{unl} + 1/3 \times \rho^{0}$).

3.2 Selection efficiencies

The selection efficiencies of these samples are respectively:

$$\left\{ \begin{array}{lcl} \varepsilon_S^{\omega} & = & 28.4 \pm .5\ \ \% \\ & & \\ \varepsilon_S^{unl} & = & 27.5 \pm .6\ \ \% \\ \varepsilon_S^{0} & = & 27.8 \pm .6\ \ \% \\ \varepsilon_S^{\rho} & = & 27.4 \pm .6\ \ \% \end{array} \right.$$

The errors correspond to the finite Monte-Carlo statistics only.
One sees some effect of the dynamics in the experimental efficiencies because $\omega\pi$ and $\rho\pi\pi$ channels show some slight differences. The difference between the 3 rho samples is merely how often the π^0, which is obviously the most difficult object to reconstruct, belongs to a ρ meson. This has probably some incidence on its detection efficiency which is however diluted by the presence of the 2 other charged pions and ends up unmeasurable.
From these results we deduce that $\varepsilon_S^{lik} \simeq \varepsilon_S^{\rho}$ and to simplify later formulae we shall take ε_S^{lik} to be equal to ε_S^0.
We have checked how the various $m_{\pi\pi}$ spectra are affected by the reconstruction and the selection process by comparing them to the KINGAL level spectra (figure 4). We observe some deficits in the reconstructed spectra in the low mass area. This is simply due to the inefficiency to reconstruct two close pions when one is a neutral (because of the cut in the distance versus energy plane against hadronic fake photons [2]) or when both have the same charge (tracking problem). This does not trouble us since we do not use the true spectra in the sequel. Rather we deduce from their similarity that we haven' t biased our spectra to the point of making our fit results irrelevant. The selection acceptance is also flat enough over the whole $m_{4\pi}$ spectrum so that our overall efficiency estimation hardly depends on the true dynamics we are trying to unveil.

3.3 ω mass cut efficiency

After the selection, we keep only those events where none of the 2 $(\pi^+\pi^-\pi^0)$ invariant masses lies between .7 and .87 GeV. We obtain for this cut only:

$$\begin{cases} \varepsilon_X^{\omega} = 6.8\ \% \\ \\ \varepsilon_X^{unl} = 83.1\ \% \\ \varepsilon_X^{0} = 66.4\ \% \\ \varepsilon_X^{\rho} = 78.4\ \% \end{cases}$$

We have been able to eliminate most of the $\omega\pi$ events at a moderate cost for our signal. One sees that ε_X^0 is now much lower than ε_X^{unl}. This is easily understood with the following argument. In the $\rho^{unl}\pi^{lik}\pi^{lik}$ subprocess, the π^{unl} and the π^0 form a ρ so that $m_{\pi^+\pi^-\pi^0} \geq m_\rho + m_\pi \geq .87\ GeV$ (upper cut limit) whereas in the 2 other subprocesses, $\rho^{lik}\pi^{unl}\pi^{lik}$ and $\rho^0\ \pi^{lik}\pi^0$, this is the case only half of the time. In the other half of the cases, only one among the 3 pions from $\pi^+\pi^-\pi^0$ belongs to a ρ so that their invariant mass tends to be lower, thus falling inside the cut range much more often. What' s more, this argument shows us that by symmetry, ε_X^{lik} must be the same as ε_X^0 which we shall henceforth hold. Since the standard $\rho\pi\pi$ current is in KORL06 made of 2/3 of $\rho^{unl}\pi^{lik}\pi^{lik}$ and 1/3 of $\rho^0\ \pi^{lik}\pi^0$ we should have: $2/3 \times \varepsilon_X^{unl} + 1/3 \times \varepsilon_X^0 = \varepsilon_X^{\rho}$. We find that $2/3 \times \varepsilon_X^{unl} + 1/3 \times \varepsilon_X^0 = 77.5 \pm 1.2\%$ and the Monte-Carlo of $\tau^\pm \rightarrow \rho\pi\pi$ yields $\varepsilon_X^{\rho} = 78.4 \pm 1.6\%$ (errors are statistical only) which is in good agreement with the previous figure.
Let us finally discuss the effect of that cut on the tau background. This point is a bit tricky because this cut is designed to remove events with an ω meson and in KORL06, the main background $\tau^\pm \rightarrow 3\pi 2\pi^0$ (40.6% of the tau background) possesses none while recent results [4] suggest it could contain as much as 80% of it. Modifying the Monte-Carlo estimate of the ω-cut efficiency for these $3\pi 2\pi^0$ events to better reflect the dynamics,

one arrives at: $\varepsilon_X^{bkg} \simeq 52.2\%$ instead of 61% by direct estimation. We will return to the uncertainty added by this manipulation in subsection 5.1.

4 Fit formulae and distributions

4.1 Fit method

We are trying to measure proportions of ρ in our sample and thus will fit the available $m_{\pi\pi}$ spectra. There are 4 of those, namely: $(\pi\pi)_{lik}$,$(\pi\pi)_{unl}$,$(\pi\pi)_{zer}$ and $(\pi\pi)_{dbl}$. This notation from now on means the spectra of invariant masses of the following C_4^2 respective subsystems of $\pi_1^{lik}\pi_2^{lik}\pi^{unl}\pi^0$:

i) $\pi_1^{lik}\pi^0$ or $\pi_2^{lik}\pi^0$

ii) $\pi^{unl}\pi^0$

iii) $\pi_1^{lik}\pi^{unl}$ or $\pi_2^{lik}\pi^{unl}$

iv) $\pi_1^{lik}\pi_2^{lik}$

Now there are 3 possible configurations for a pair of pions according to how many of them belong to a ρ meson. If both, the mass spectrum is a ρ Breit-Wigner we shall name $[ins]$, if one it is a phase-space like spectrum called $[mix]$, if none it is a similar one (though more strongly pushed to lower invariant masses than the previous because it lives together with a resonant ρ) called $[ext]$ for obvious reasons (see figure 3).
The procedure consists in fitting simultaneously the 4 $m_{\pi\pi}$ spectra with the 3 reference distributions [ins],[mix] and [ext]. This will yield the desired proportions of the 3 different ρs in the $\rho\pi\pi$ channel if we neglect the effect of possible interferences. To see that, let us first detail the content of each subprocess in terms of the 4 $m_{\pi\pi}$ combinations:

1. ρ^{unl}: $(\pi\pi)_{unl} = [ins], (\pi\pi)_{dbl} = [ext]$ *and* $(\pi\pi)_{lik} = (\pi\pi)_{zer} = 2 \times [mix]$
2. ρ^{lik}: $(\pi\pi)_{unl} = (\pi\pi)_{dbl} = [mix], (\pi\pi)_{lik} = [ins] + [mix]$ *and* $(\pi\pi)_{zer} = [ext] + [mix]$
3. ρ^{zer}: $(\pi\pi)_{unl} = (\pi\pi)_{dbl} = [mix], (\pi\pi)_{lik} = [ext] + [mix]$ *and* $(\pi\pi)_{zer} = [ins] + [mix]$

Note that the reference distributions are normalised to represent one entry per candidate which explains the factor 2 in front of some $(\pi\pi)$ combinations. These formulae show how we obtain our reference distributions with the 2 special Monte-Carlo ρ^{unl} and ρ^0.
Now we assume that $\tau^\pm \to \rho\pi\pi$ is a linear incoherent superposition of the 3 subprocesses $\tau^\pm \to \rho^{unl}\pi^{lik}\pi^{lik}$,$\tau^\pm \to \rho^{lik}\pi^{unl}\pi^{lik}$ and $\tau^\pm \to \rho^0\ \pi^{lik}\pi^0$ with respective weights W_{unl},W_{lik} and W_{zer}. This yields the formulae:

$$\begin{cases} (\pi\pi)_{unl} & \propto & W_{unl} \times [ins] + W_{lik} \times [mix] + W_{zer} \times [mix] \\ (\pi\pi)_{lik} & \propto & 2W_{unl} \times [mix] + W_{lik} \times ([ins] + [mix]) + W_{zer} \times ([ext] + [mix]) \\ (\pi\pi)_{zer} & \propto & 2W_{unl} \times [mix] + W_{lik} \times ([ext] + [mix]) + W_{zer} \times ([ins] + [mix]) \\ (\pi\pi)_{dbl} & \propto & W_{unl} \times [ext] + W_{lik} \times [mix] + W_{zer} \times [mix] \end{cases}$$

We assume implicitly that $W_{unl} + W_{lik} + W_{zer} \equiv 100\%$ and thus, fitting the shapes of the spectra, we have only 2 free parameters. We may of course choose any parametrisation we like. Because the ρ^{unl} situation stands apart from that of ρ^{lik} and ρ^0, we replace W_{unl} by $1 - W_{lik} - W_{zer}$. Furthermore, since in our fit these 2 weights are correlated at the 50% level, we prefer using as variables their sum $\Sigma \equiv W_{lik} + W_{zer}$ and difference $\Delta \equiv W_{lik} - W_{zer}$ which are uncorrelated (correlation below 1.2%). This will prove easier later when computing the errors on the weights. The corresponding formulae read:

$$\begin{cases} (\pi\pi)_{unl} & \propto \quad \Sigma \times [mix] + (1-\Sigma) \times [ins] \\ (\pi\pi)_{dbl} & \propto \quad \Sigma \times [mix] + (1-\Sigma) \times [ext] \\ (\pi\pi)_{lik} & \propto \quad (2-\Sigma) \times [mix] + (\Sigma+\Delta)/2 \times [ins] + (\Sigma-\Delta)/2 \times [ext] \\ (\pi\pi)_{zer} & \propto \quad (2-\Sigma) \times [mix] + (\Sigma-\Delta)/2 \times [ins] + (\Sigma+\Delta)/2 \times [ext] \end{cases}$$

Let us now perform that fit and correct it for successively tau contamination, ω background and ω mass cut efficiencies.

4.2 Successive fits

To demonstrate the consistency of the method, we perform the global fit (using simultaneously the four above equations) on successively raw, cleaned from τ background and cleaned from τ and $\omega\pi$ background $(\pi\pi)$ distributions. Finally, we correct for the difference in the efficiencies.

- On the whole selected sample with τ and $\omega\pi$ contamination, we obtain the following result (figure 5):

  $$\begin{cases} \Sigma & = \quad 67.5 \pm 2.6 \quad \% \\ \Delta & = \quad 5.5 \pm 5.4 \quad \% \end{cases}$$

  This translates for the original weights into:

  $$\begin{cases} W_{lik} & = \quad 36.5 \pm 3.0 \quad \% \\ W_{zer} & = \quad 31.0 \pm 3.0 \quad \% \end{cases}$$

  And subsequently (sum is constrained to 1):

  $$W_{unl} = 32.5 \pm 2.8\%$$

  Note that the different errors are correlated by this constraint.

- Let us subtract the estimated τ background from the $m_{\pi\pi}$ spectra (figure 6). The contamination amounts to (see 3.3):

  $$c_{bkg} = 14.8\%$$

  One can see that, understandably, this background mainly contributes to the ρ^0 peak and we thus expect W_{zer} to decrease. Furthermore it is completely devoid of ρ^{unl} and hence the new $(\pi\pi)_{unl}$ mass spectrum has a much lower low mass tail which should increase W_{unl}. Indeed we obtain (figure 7):

  $$\begin{cases} W_{lik} & = \quad 35.7 \pm 3.2 \quad \% \\ W_{zer} & = \quad 23.2 \pm 3.2 \quad \% \\ W_{unl} & = \quad 41.1 \pm 3.0 \quad \% \end{cases}$$

- Let us now correct for the remnant of $\omega\pi$ events. As explained in 3.1, we are rather confident in the subtraction process. If we assume that $\omega\pi$ and $\rho\pi\pi$ saturate the $3\pi\pi^0$ channel, the estimated contamination (after τ subtraction) , shown on figure 8, is:

$$c_{\omega\pi} = \frac{1}{1 + \frac{(1-\alpha)\ \varepsilon^{\rho}}{\alpha\ BR(\omega \to \pi^+\pi^-\pi^0)\ \varepsilon^{\omega}}} = 7.6\%$$

(in which $\alpha \equiv \frac{\Gamma(\tau\to\omega\pi)}{\Gamma(\tau\to 3\pi\pi^0)}$)

The result of the fit is now:

$$\begin{cases} W_{lik} &= 31.5 \pm 3.4 \ \% \\ W_{zer} &= 19.4 \pm 3.4 \ \% \\ W_{unl} &= 49.1 \pm 3.1 \ \% \end{cases}$$

As before, we increase our statistical error according to the loss in statistics in our $m_{\pi\pi}$ spectra. We have checked that the error varies identically if instead of subtracting these events, we keep them and fit in presence of the corresponding background. The error growth is then not due to a statistical loss but to the presence of a fixed background that diminishes the separation power of the fit.

- Eventually, we correct the formulae by the efficiency ratio between $\rho^{unl}\pi^{lik}\pi^{lik}$ and $\rho^0\ \pi^{lik}\pi^0$. Because of the anti-ω cut we have (see 3.3):

$$A \equiv \frac{\varepsilon^{unl}}{\varepsilon^{zer}} (= \frac{\varepsilon^{unl}}{\varepsilon^{lik}}) \simeq 1.24$$

Thus the corrected formulae read:

$$\begin{cases} (\pi\pi)_{unl} & \propto \ \Sigma \times [mix] + A \times (1-\Sigma) \times [ins] \\ (\pi\pi)_{dbl} & \propto \ \Sigma \times [mix] + A \times (1-\Sigma) \times [ext] \\ (\pi\pi)_{lik} & \propto \ (\Sigma + 2A \times (1-\Sigma)) \times [mix] + (\Sigma+\Delta)/2 \times [ins] + (\Sigma-\Delta)/2 \times [ext] \\ (\pi\pi)_{zer} & \propto \ (\Sigma + 2A \times (1-\Sigma)) \times [mix] + (\Sigma-\Delta)/2 \times [ins] + (\Sigma+\Delta)/2 \times [ext] \end{cases}$$

From these we expect W_{lik}/W_{zer} to remain unaltered and W_{unl} to decrease (because $A > 1$). Indeed we get (figure 9):

$$\boxed{\begin{cases} W_{lik} &= 34.8 \pm 3.4 \ \% \\ W_{zer} &= 21.4 \pm 3.4 \ \% \\ W_{unl} &= 43.8 \pm 3.1 \ \% \end{cases}}$$

This is our final result. Let us now perform all necessary systematic checks.

5 Systematic errors

We have eventually 3 inputs in our fit: c_{bkg}, $c_{\omega\pi}$ and $A \equiv \frac{\varepsilon^{unl}}{\varepsilon^{zer}}$. Their uncertainties translate into 3 different systematic errors. As for the tau background, we will also assign a systematic error to its composition and dynamics lack of knowledge. We also have an error coming from the fit itself (binned maximum 0 method). Last and more difficult, we attempt to estimate 2 theoretical problems: the effect of neglecting all interferences between the 3 ρs and that of ignoring the exact dynamics. For this last issue, we investigate as an example the effect of taking the $(\pi - \pi)_s$ systems as non-interacting.

5.1 τ Background

Overall background level:

The error on $c_{bkg} = 14.8\%$ comes from the limited Monte-Carlo statistics as well as from the uncertainties on the dominant background channel branching fractions:

$$\begin{cases} BR(\tau^{\pm} \to 3\pi 2\pi^0) & = & 0.48 \pm .06 & \% & [4] \\ BR(\tau^{\pm} \to 3\pi) & = & 9.56 \pm .32 & \% & \text{Aleph Ohio workshop} \end{cases}$$

We obtain $\Delta(c_{bkg})/c_{bkg} = 5.3_{statMC} \oplus 3.6_{\Delta(BR)}\%$ which yields:

$$\begin{cases} \Delta(W_{lik}) & = & .2 & \% \\ \Delta(W_{zer}) & = & 1.3 & \% \\ \Delta(W_{unl}) & = & 1.5 & \% \end{cases}$$

Background composition:

The main uncertainty is how much of the remaining tau background comes from $3\pi 2\pi^0$ events. From [4] we have $\Delta(BR)/BR = 12.5\%$ and from our problem in estimating $\varepsilon_X^{3\pi 2\pi^0}$ (3.3) we deduce $\Delta(\varepsilon_X)/\varepsilon_X \simeq 10\%$. Varying the $3\pi 2\pi^0$ proportion within 16% we obtain:

$$\begin{cases} \Delta(W_{lik}) & = & .8 & \% \\ \Delta(W_{zer}) & = & .1 & \% \\ \Delta(W_{unl}) & = & .7 & \% \end{cases}$$

Background dynamics:

We know that the $m_(\pi\pi)$ spectra for $3\pi 2\pi^0$ are sensibly wrong. On the other hand they represent a very low statistics and, by comparison to $\omega\pi$, are not expected to be very sharply peaked so that this defect's influence on the fitted weights can be neglected.

5.2 $\omega\pi$ background

As mentioned, this channel's dynamics is well established and we need only consider the error on its remaining proportion. From the formula of subsection 4.2 we get:

$$\Delta(c_{\omega\pi})/c_{\omega\pi} = r/(1+r) \times (\ \Delta(\varepsilon^{\rho})/\varepsilon^{\rho} \oplus \Delta(\varepsilon^{\omega})/\varepsilon^{\omega} \oplus \Delta(B_{\omega})/B_{\omega} \oplus \Delta\alpha/\alpha(1-\alpha)\ )$$

where ε are the overall efficiencies, r means $1/c_{\omega\pi} - 1$, $\alpha = \frac{\Gamma(\tau \to \omega\pi)}{\Gamma(\tau \to 3\pi\pi^0)}$ and $B_{\omega} = 88.8 \pm .6\%$. From Monte-Carlo statistics we have: $\Delta(\varepsilon^{\rho})/\varepsilon^{\rho} = 3\%$ and $\Delta(\varepsilon^{\omega})/\varepsilon^{\omega} = 6\%$

From [2] we have $\Delta\alpha/\alpha(1-\alpha) = 14\%$
We obtain $\Delta(c_{\omega\pi})/c_{\omega\pi} = 16\%$ and implementing this in our fit:

$$\begin{cases} \Delta(W_{lik}) &= .5 \ \% \\ \Delta(W_{zer}) &= .7 \ \% \\ \Delta(W_{unl}) &= .9 \ \% \end{cases}$$

5.3 Efficiency ratio

The last input is the ratio $A = \frac{\epsilon^{unl}}{\epsilon^{zer}}$ which corrects our fit formulae. From our limited Monte-Carlo statistics we deduce $\Delta(A)/A = 3\%$ which yields:

$$\begin{cases} \Delta(W_{lik}) &= 1.0 \ \% \\ \Delta(W_{zer}) &= 0.6 \ \% \\ \Delta(W_{unl}) &= 1.6 \ \% \end{cases}$$

5.4 Binning and range

If we change the number of bins between 25 and 40, we get the following variations:

$$\begin{cases} \Delta(W_{lik}) &= 0.8 \ \% \\ \Delta(W_{zer}) &= 1.1 \ \% \\ \Delta(W_{unl}) &= 1.9 \ \% \end{cases}$$

Cutting the edges of the mass spectra more or less strictly yields:

$$\begin{cases} \Delta(W_{lik}) &= 1.4 \ \% \\ \Delta(W_{zer}) &= 1.4 \ \% \\ \Delta(W_{unl}) &= 2.2 \ \% \end{cases}$$

These errors are rather large because when grinding at the inside of the distributions, one does no longer fit exactly the same quantities. The proportions fitted are now those in the remaining part of the spectra which are not generally those of the whole spectra. This makes the above values quite conservative.

5.5 Interference effects

Let us fit the full $\rho\pi\pi$ Monte-Carlo with our method. If our fit works well we should find the true (MC) proportions of KORL06 i.e. :

$$\begin{cases} W_{lik}^{MC} &= 0 \\ W_{zer}^{MC} &= 1/3 \\ W_{unl}^{MC} &= 2/3 \end{cases}$$

Any deviation will be a sign of interference effects since no background of τ or $\omega\pi$ enters here. We should also see on the fitted shapes whether they can be adjusted to look like the true ones or whether no simple linear superposition can be made to reproduce the full spectra. Our fit gives:

$$\begin{cases} \Sigma &= 36.7 \pm 1.4 \quad \% \\ \Delta &= -32.0 \pm 2.9 \quad \% \end{cases}$$

That is:

$$\begin{cases} W_{lik} & = \ 2.3 \pm 1.6 \ \ \% \\ W_{zer} & = \ 34.3 \pm 1.6 \ \ \% \\ W_{unl} & = \ 63.3 \pm 1.4 \ \ \% \end{cases}$$

Figure 10 shows that the $(\pi\pi)_{lik}$ and $(\pi\pi)_{zer}$ mass spectra are fairly well reproduced. The double charged mass spectrum however tends to have lower mass in the full Monte-Carlo where the current is correctly symmetrized. This is also visible on the data (figure 9) and points to a Bose-Einstein correlations related effect. The shaded spectrum indeed is a linear superposition of reference distributions which by construction are not symmetrized. Yet this distortion is of very small impact on the fit itself.
This effect is probably also responsible for the shift between the two ρ peaks in the $(\pi\pi)_{unl}$ mass spectra in the Monte-Carlo because this combination of pions is the one living together with the $(\pi\pi)_{dbl}$ couple. This shift is responsible for most of the 5% relative error on W_{unl} but is not observed in the data and thus we estimate a smaller systematic error on W_{unl}.
Finally, the rather large error on W_{lik} is due to the fact that it is null in the Monte-Carlo. A larger weight, like W_{zer}, is better fitted because the higher the ρ peak, the easier the fit. One indeed sees that a 2.3% weight is indistinguishable from 0 (the true value) on the second plot of figure 10. For this reason we estimate systematic errors from interference effects on W_{lik} and W_{zer} proportional to these weights themselves.
We find:

$$\begin{cases} \Delta(W_{lik}) & \simeq \ 1.0 \ \ \% \\ \Delta(W_{zer}) & \simeq \ 1.5 \ \ \% \\ \Delta(W_{unl}) & \simeq \ 2.0 \ \ \% \end{cases}$$

5.6 Dynamics of the $\rho\pi\pi$ channel

We do not know the exact matrix element for this final state. In particular, the model [1] takes all s-wave $(\pi - \pi)$ systems as non-interacting. Let us take this approximation as an example of the effect of the unknown dynamics.
In $\rho^{unl}\pi^{lik}\pi^{lik}$ and $\rho^0\ \pi^{lik}\pi^0$ we must have the following isospin-orbital momentum configuration:

$$\left[\overbrace{\begin{array}{cc} (\overset{p}{\widehat{\pi - \pi}})^{unl} & (\overset{s}{\widehat{\pi^{lik} - \pi^{lik}}}) \\ \underbrace{(\overset{p}{\widehat{\pi - \pi}})^{zer}}_{I=1} & \underbrace{(\overset{s}{\widehat{\pi^{lik} - \pi^{zer}}})}_{I=2} \end{array}}^{s} \right.$$

In $\rho^{lik}\pi^{unl}\pi^{lik}$ however, the s-wave $(\pi^{unl} - \pi^{lik})$ can be either in total isospin I=2 or <u>I=0</u> (because $I_3 = 0$) which changes its mass spectrum. It is known indeed that the phase shift is much larger for an I=0 $(\pi - \pi)_s$ system than for I=2. This difference could be responsible for the shifting of the ρ^{lik} peak towards lower masses than either the ρ^{unl} or the ρ^{zer} peaks (around 700 MeV instead of 730). This shift can be observed on the data. If we try to correct for this by fitting the $(\pi\pi)_{lik}$ spectrum with an [ins] (Breit-Wigner) distribution shifted by 30 MeV, we get:

$$\begin{cases} \Sigma & = \ 56.8 \pm 3.1 \ \ \% \\ \Delta & = \ 16.8 \pm 6.2 \ \ \% \end{cases}$$

That is:

$$\begin{cases} W_{lik} &= 36.8 \ \% \\ W_{zer} &= 20.0 \ \% \\ W_{unl} &= 43.2 \ \% \end{cases}$$

We thus assign to this shortcoming of the Monte-Carlo the approximate systematic errors:

$$\begin{cases} \Delta(W_{lik}) &\simeq 2 \ \% \\ \Delta(W_{zer}) &\simeq 1.4 \ \% \\ \Delta(W_{unl}) &\simeq .6 \ \% \end{cases}$$

W_{lik} is not alone to receive corrections because in our global way to fit, the 2 parameters fitted are not independent. We do not show the plots of that fit since they look much like the normal one.

5.7 Conclusion

Let us sum up the systematics:

	$\Delta(W_{lik})$ (%)	$\Delta(W_{zer})$ (%)	$\Delta(W_{unl})$ (%)
c_{bkg}	.2	1.3	1.5
$N_{3\pi 2\pi^0}$	.8	.1	.7
$c_{\omega\pi}$	.5	.7	.9
A	1.	.6	1.6
Binning	1.4	1.4	2.2
Interference	1.	1.5	2.
$I = 0 \ (\pi - \pi)_s$	2.	1.4	.6
SUM	**3.0**	**3.0**	**3.9**

We have arrived at the following proportions of the 3 possible ρs inside $\rho\pi\pi$:

$$\begin{cases} W_{lik} &= 34.8 \pm 3.4_{stat} \pm 3.0_{syst} \ \% \\ W_{zer} &= 21.4 \pm 3.4_{stat} \pm 3.0_{syst} \ \% \\ W_{unl} &= 43.8 \pm 3.1_{stat} \pm 3.9_{syst} \ \% \end{cases}$$

The ARGUS [3] result reads:

$$\begin{cases} W_{lik} &= 40.6 \pm 7.8_{stat} \pm 1.6_{syst} \ \% \\ W_{zer} &= 46.9 \pm 6.3_{stat} \pm 3.1_{syst} \ \% \\ W_{unl} &= 15.6 \pm 4.7_{stat} \pm 0.6_{syst} \ \% \end{cases}$$

One sees that the $\rho^{lik}\pi^{unl}\pi^{lik}$ fractions are in rough agreement but the two others strongly disagree. The statistics of this study is about three times larger than [3] but their paper is not detailed enough to make more precise statements.

6 $(\rho-\rho)_p$ channel

6.1 Introduction

We have explained in chapter 1 why this channel is strongly suppressed compared to $\rho\pi\pi$. It is uneasy to quantify this statement. We do not have any Monte-Carlo generator producing this kind of final state. Since we are at the limit of the phase-space, one might wonder what the ρ resonances would look like, at which mass they should peak, what are the corresponding reference distributions... If we want to perform on these events a fit similar to that used for $\rho\pi\pi$, one might also ask how these events can be separated and what then would be the remaining background (mainly from $\rho\pi\pi$). Furthermore, if we cut on $(\pi\pi)_{lik}$ around the ρ^{lik} peak ($\sim$ 700 MeV), the other 2 pions, in a $\rho\pi\pi$ decay, are precisely those of total isospin I=0 or 2 which tend to have a higher invariant mass and thus to look more like a ρ peak, expected for a $(\rho-\rho)_p$ decay, than the I=2 $(\pi\pi)_s$ systems...

6.2 First glance

To get a first feel of the importance of a possible $(\rho-\rho)_p$ presence, the natural thing to do is plotting one ρ mass versus the corresponding other and see whether the (m_ρ, m_ρ) area is more populated than its surroundings. We look at this using data after selection and $\omega\pi$ and τ background subtraction. We also look at the projections of this 2D-plot and compare them with that of the bands which should contain the $(\rho-\rho)_p$ events. This is shown on figure 11. We have taken from our result on $\rho\pi\pi$ the ρ^{lik} peak to lie between 620 and 780 MeV and the ρ^0 between 650 and 810 MeV. The 2D-plot doesn' t show a large enhancement in the (m_ρ, m_ρ) area and the projections have a statistics too low to draw any meaningful quantitative conclusion.

6.3 Comparison to $\rho\pi\pi$

Now we would like to fit the $(\rho-\rho)_p$ the same way we just did for $\rho\pi\pi$. This will not yield reliable estimates because of the afore mentioned problems but should give us a hint on the relative contributions. We have to do rough approximations like using the same reference distributions, adapting the background and $\omega\pi$ subtractions ... We also restrict ourselves to using only the $(\pi\pi)_{lik}$ and $(\pi\pi)_{zer}$ distributions for both fits because they are the relevant ones for $(\rho-\rho)_p$ and we do not know how the 2 others would be for such events.

- First we redo the final fit using only those 2 spectra, we get:

$$\begin{cases} \Sigma &= 68.6 \pm 7.8 \ \% \\ \Delta &= 13.7 \pm 6.0 \ \% \end{cases}$$

  As mentioned, Σ is essentially fitted by $(\pi\pi)_{unl}$ and hence poorly determined here.

- Second we adapt this procedure to fit the shaded histograms of figure 11 i.e. the same $(\pi\pi)$ spectra but after cutting on the corresponding second $(\pi\pi)$ combination to select a ρ. We expect to obtain $\Delta' \equiv 0$ and $\Sigma' \equiv 2 \times W_{\rho\rho}$ since now W_{lik} and W_{zer} both mean $W_{\rho\rho}$. We find:

$$\begin{cases} \Sigma' &= 14.8 \pm 16.8 \quad \% \\ \Delta' &= 2.3 \pm 11.7 \quad \% \end{cases}$$

Δ' is indeed close to 0 and $W_{\rho\rho} \simeq 7.5 \pm 8.4\%$ which is also compatible with a complete absence of $(\rho - \rho)_p$

This certainly does not yield the proportion of $(\rho - \rho)_p$ but simply indicates a much lower contribution than that of $\rho\pi\pi$. In this work where the relative precisions, both statistical and systematic, are around 15%, we can live with this imprecision.

7 Conclusion

We have shown that the $\tau^\pm \to 3\pi\pi^0$ decay can be described in terms of non-interfering $\tau^\pm \to \rho^{unl}\pi^{lik}\pi^{lik}$, $\tau^\pm \to \rho^{lik}\pi^{unl}\pi^{lik}$ and $\tau^\pm \to \rho^0\ \pi^{lik}\pi^0$ (and $\tau^\pm \to \omega\pi$) subprocesses. Their relative proportions have been determined to be respectively: $W_{unl} = 43.8\%$, $W_{lik} = 34.8\%$ and $W_{zer} = 21.4\%$ with a relative precision between 11 and 20% (increasing when W decreases). These 3 weights represent 49% of the whole $\tau^\pm \to 3\pi\pi^0$ decay. The rest is made of $\omega\pi$ and possibly of a small amount of $(\rho - \rho)_p$ decays.
From [2] we had already [1]:

$$Br(\tau^\pm \to \omega\pi^\pm\nu_\tau) = 2.15 \pm .18\%$$

So that $\rho\pi\pi$ represents:

$$Br(\tau^\pm \to \rho\pi\pi\nu_\tau) \simeq 2.1\%$$

This kind of study will benefit a lot from more statistics but shall also need new Monte-Carlo generators to improve sensibly. It would be also interesting to study the related $\tau^\pm \to \pi^\pm 3\pi^0$ decay to complement our approach. The results presented here, at least for the $\rho^{unl}\pi^{lik}\pi^{lik}$ and $\rho^0\ \pi^{lik}\pi^0$ proportions, are very different from those of ARGUS [3].

[1]This value is also slightly altered because of the correction on α mentioned in 2.1

References

[1] R. Fisher, J. Wess and R. Wagner, Z Phys C3 313 (1980)

[2] P. Bourdon: Measurement of $\tau \rightarrow 3\pi\pi^0$ branching ratio and study of the ω production, Aleph note 94-024

[3] ARGUS collaboration, PL B260 259 (1991)

[4] CLEO collaboration, PRL 71 12 (1993)

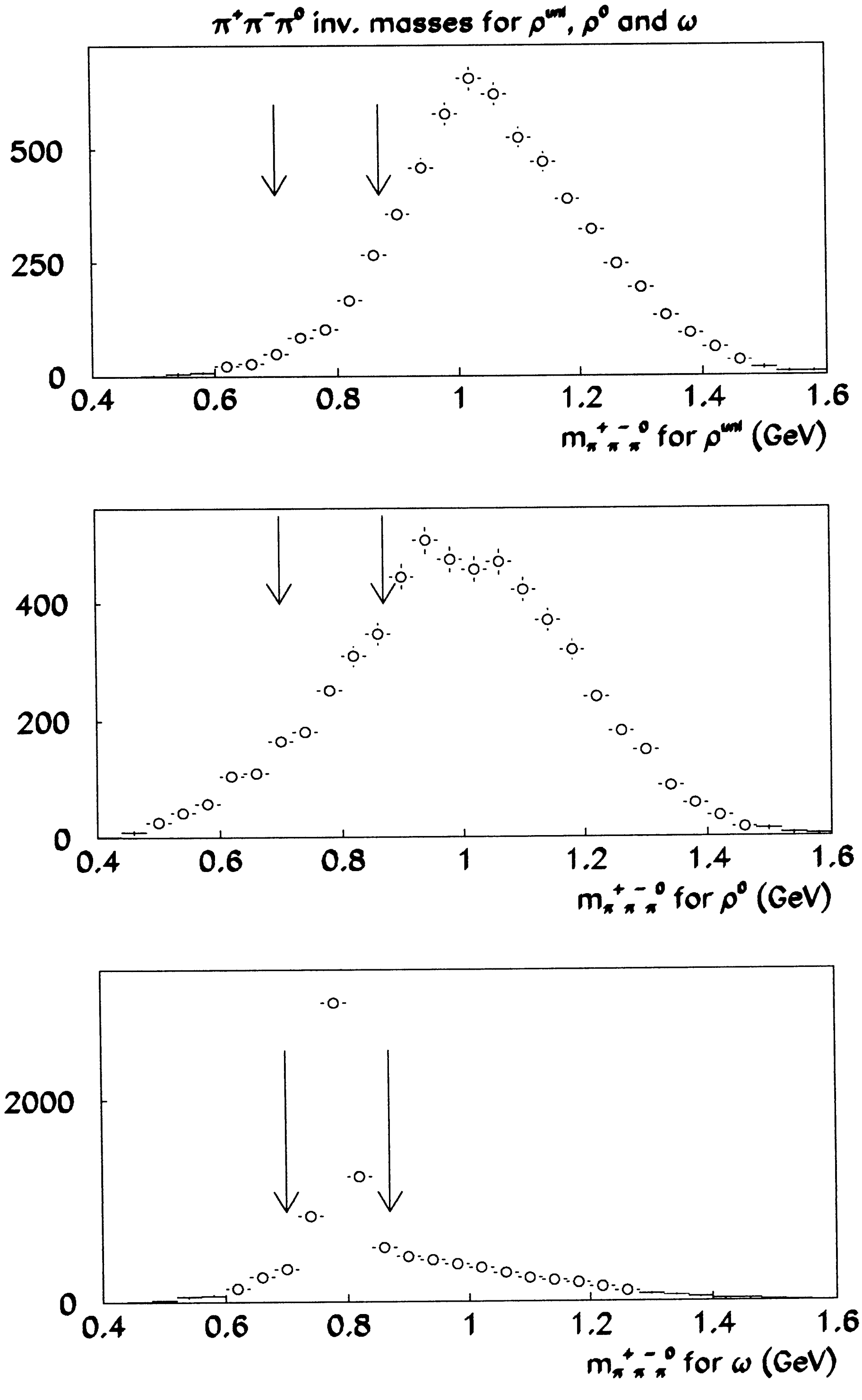

Figure 1: $\omega\pi$ invariant masses for the relevant Monte-Carlo samples. The cut zone is indicated by the arrows

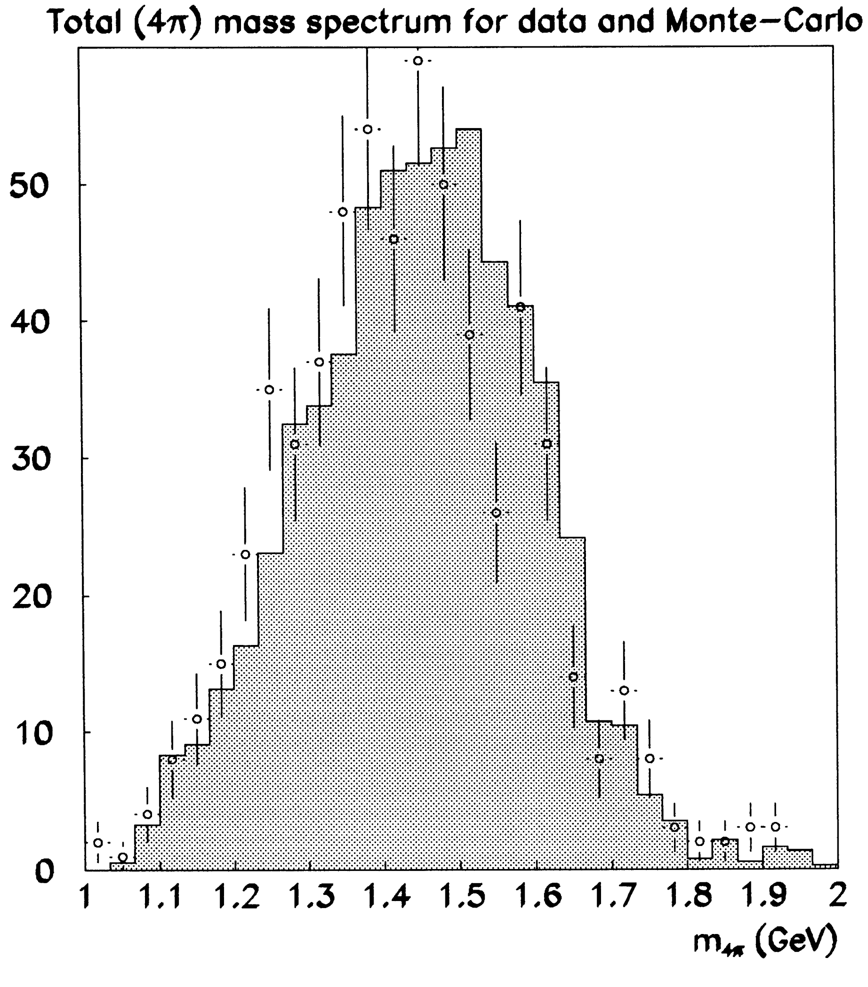

Figure 2: The $\rho\pi\pi$ invariant mass of the data (dots) is more or less reproduced by the Monte-Carlo (shaded). No large bias on the $m_{\pi\pi}$ spectra is expected.

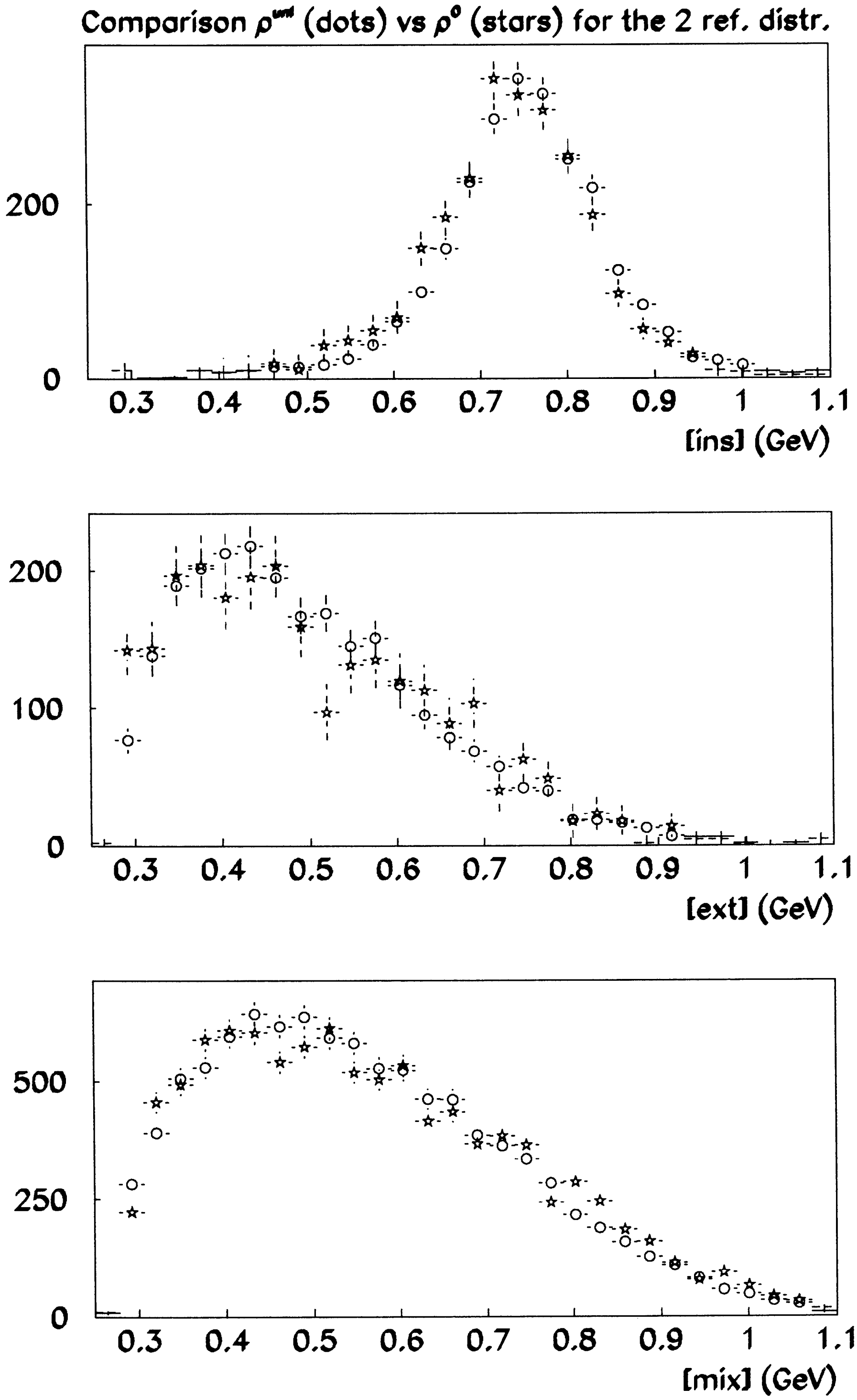

Figure 3: The reference distributions obtained from the pure ρ^{unl} and the pure ρ^0 Monte-Carlo are in good agreement and can be combined

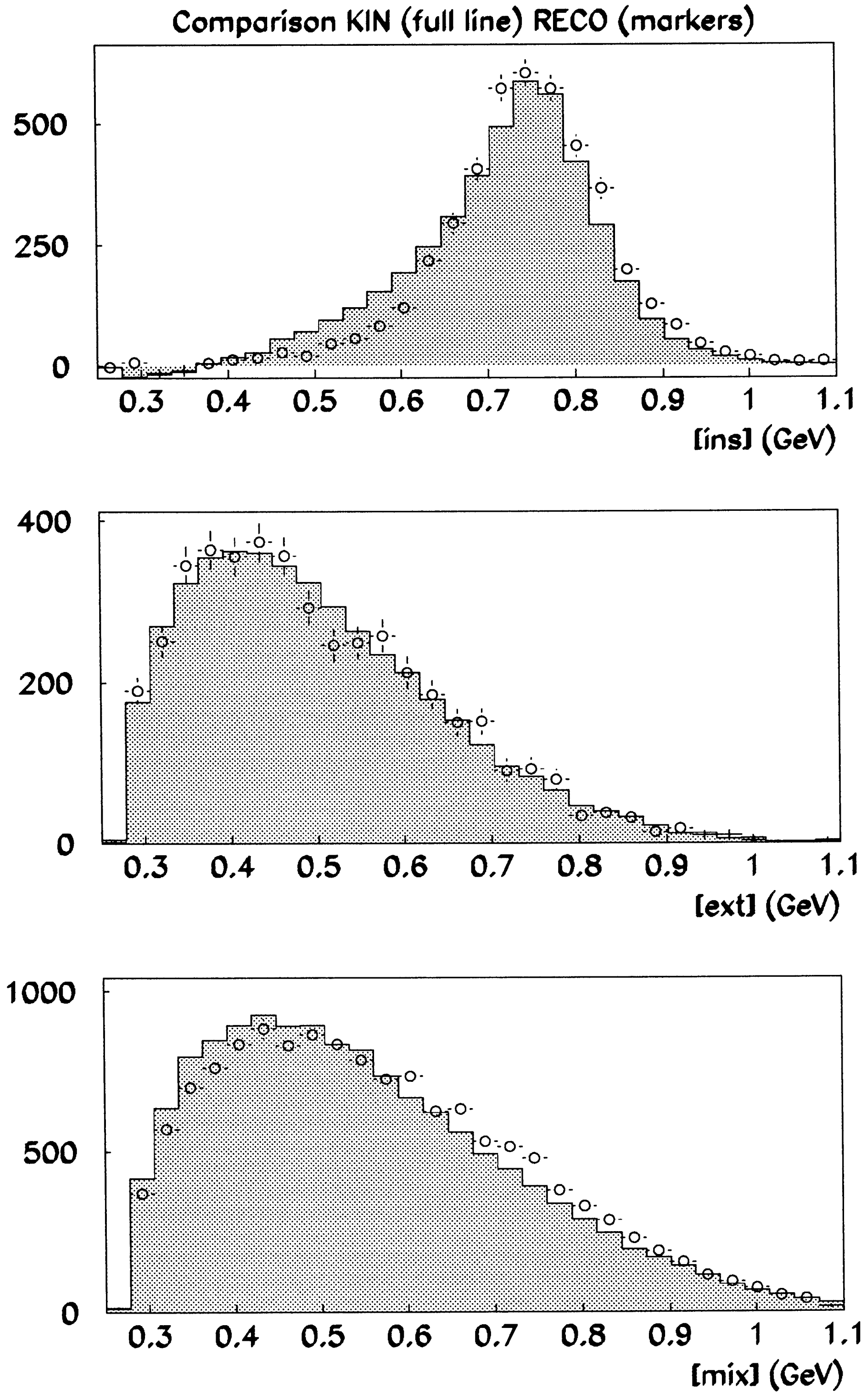

Figure 4: The true Monte-Carlo shapes (full line) are essentially preserved by the reconstruction and selection processes (dots)

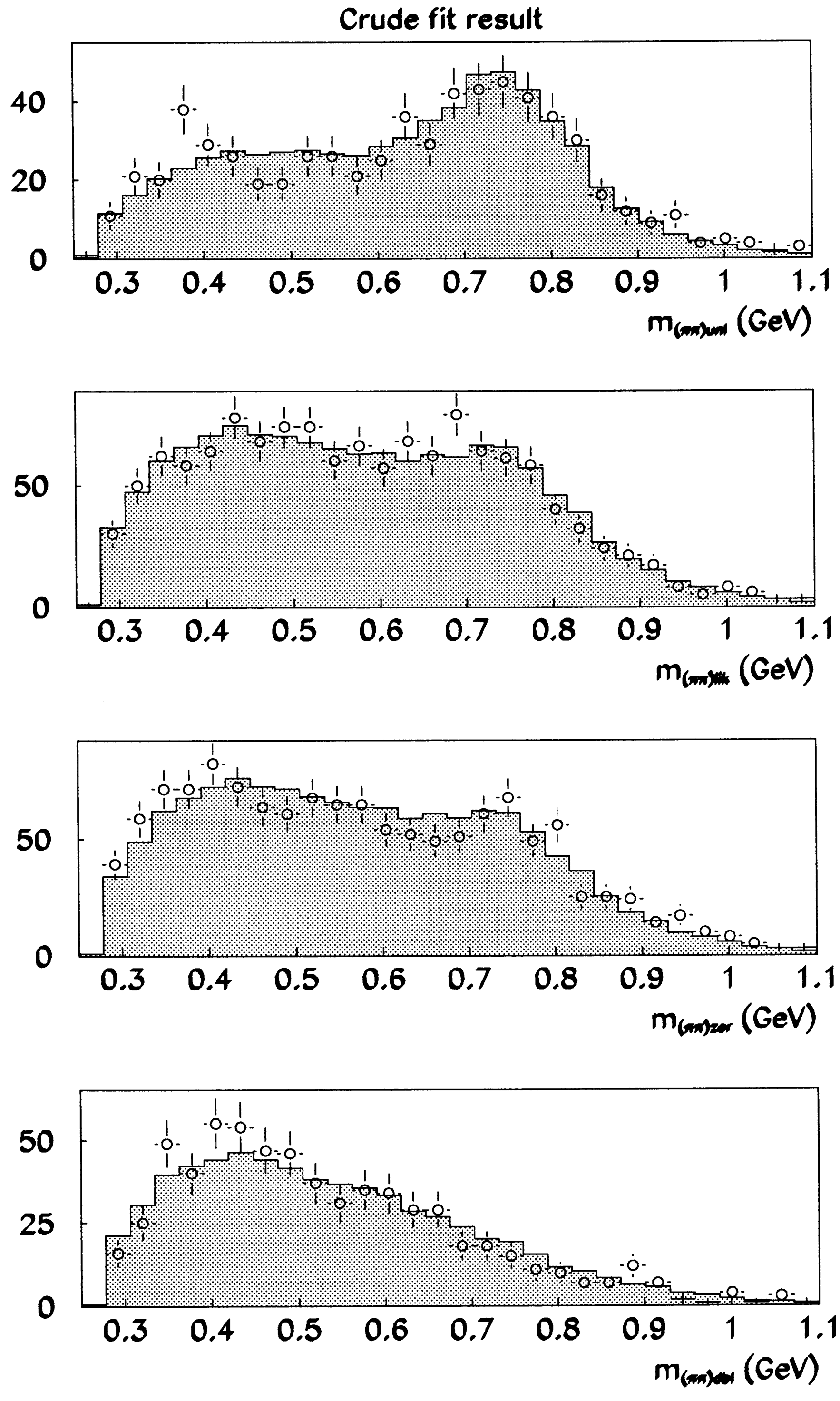

Figure 5: Raw $m_{(\pi\pi)}$ spectra (dots) and results of the fit (shaded) show a satisfactory agreement for all of the existing combinations (unlike, like, neutral and doubly charged from top to bottom)

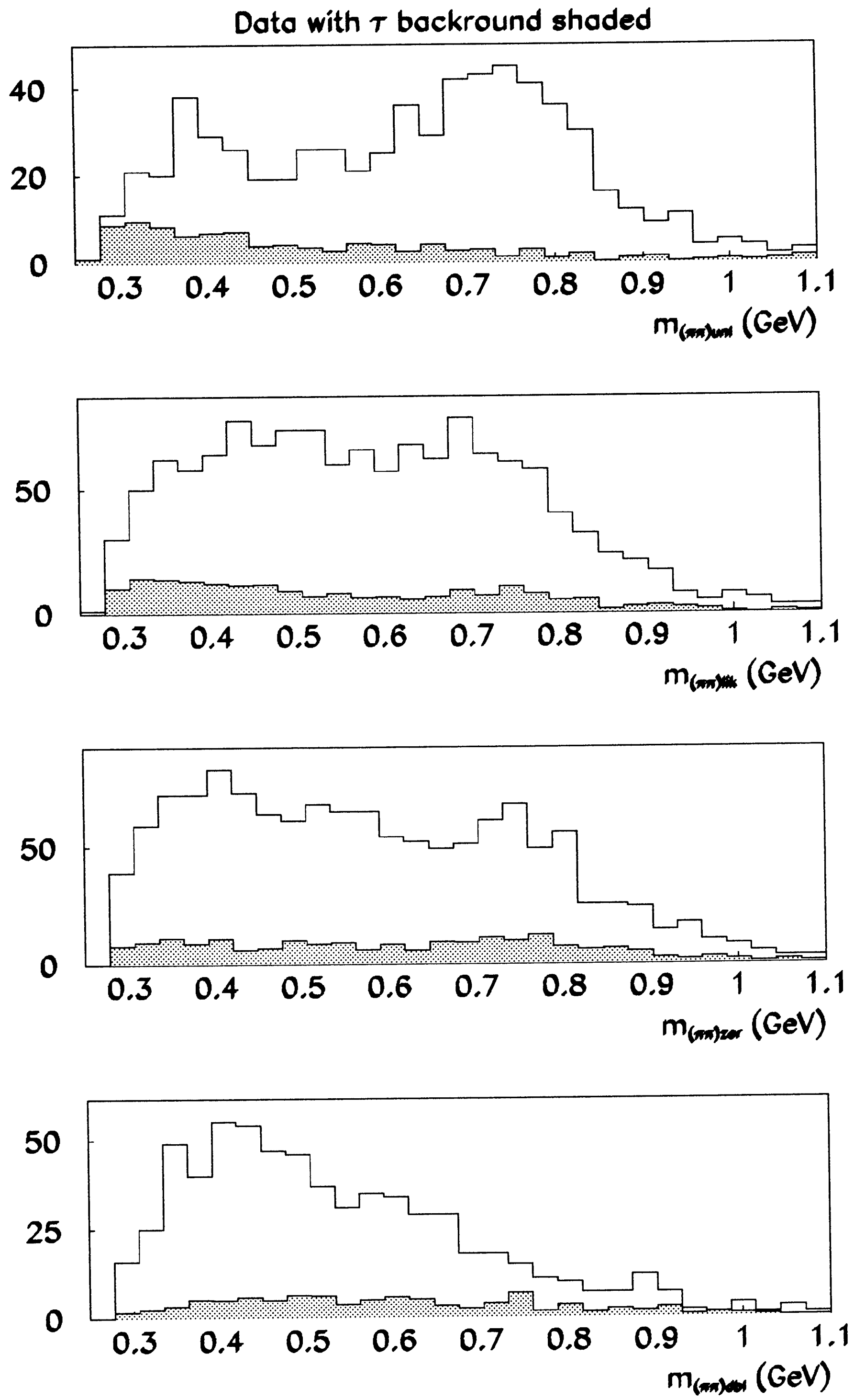

Figure 6: The τ background contribution to the various $m_(\pi\pi)$ spectra (shaded)

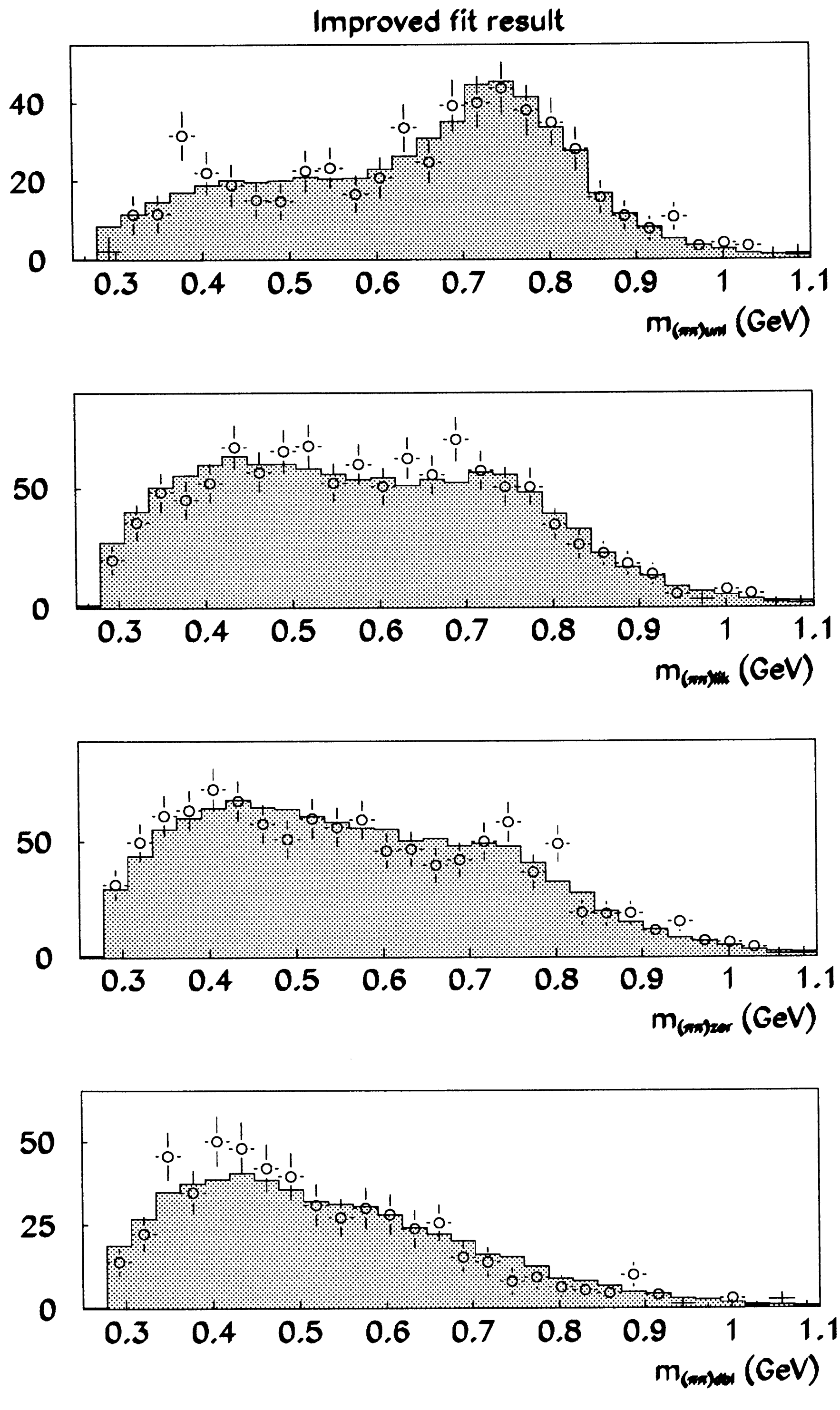

Figure 7: Same as previous fit results but the background shown opposite has been subtracted

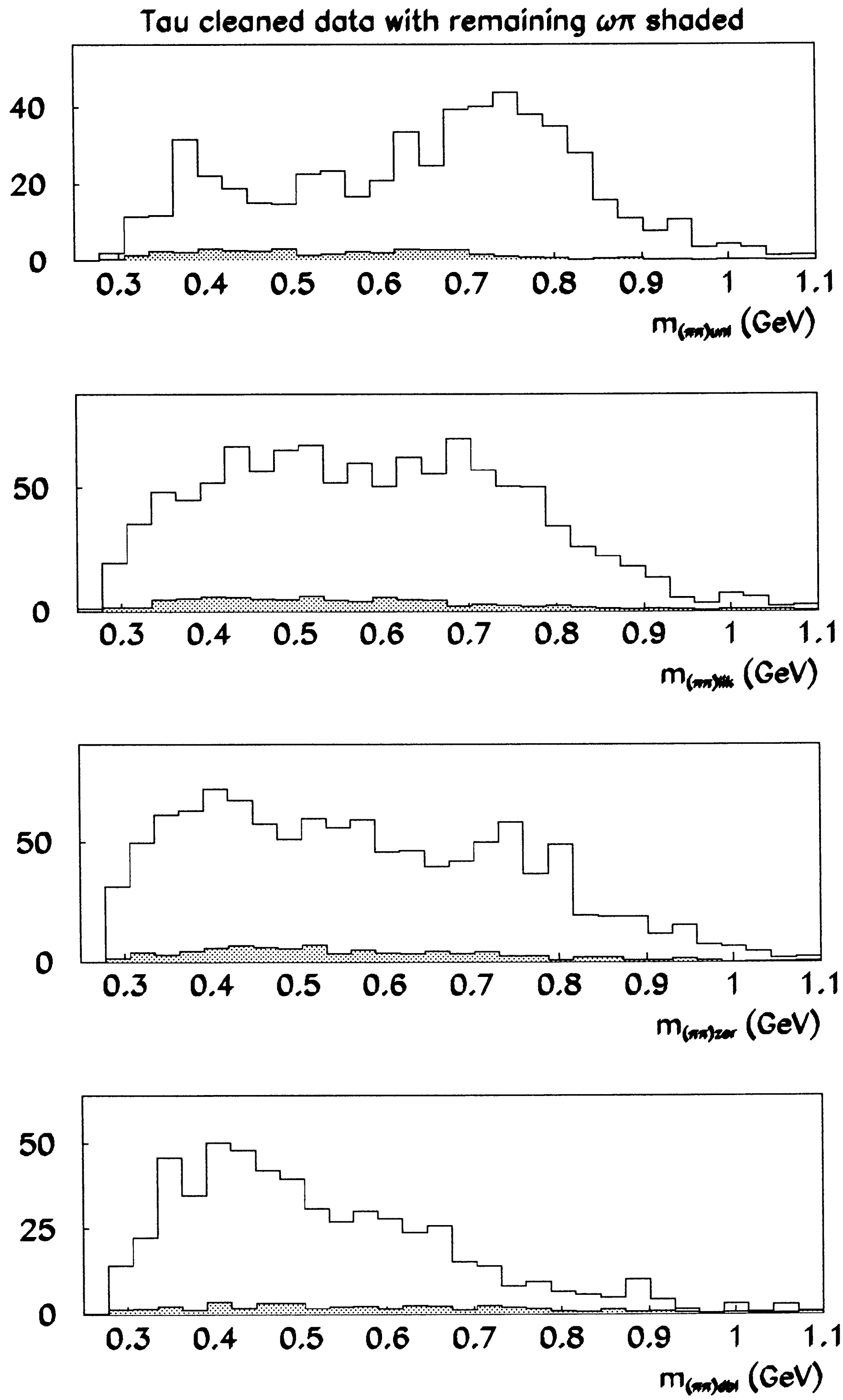

Figure 8: The remaining background of $\omega\pi$ events (shaded) contribution to the various $m_{(\pi\pi)}$ spectra

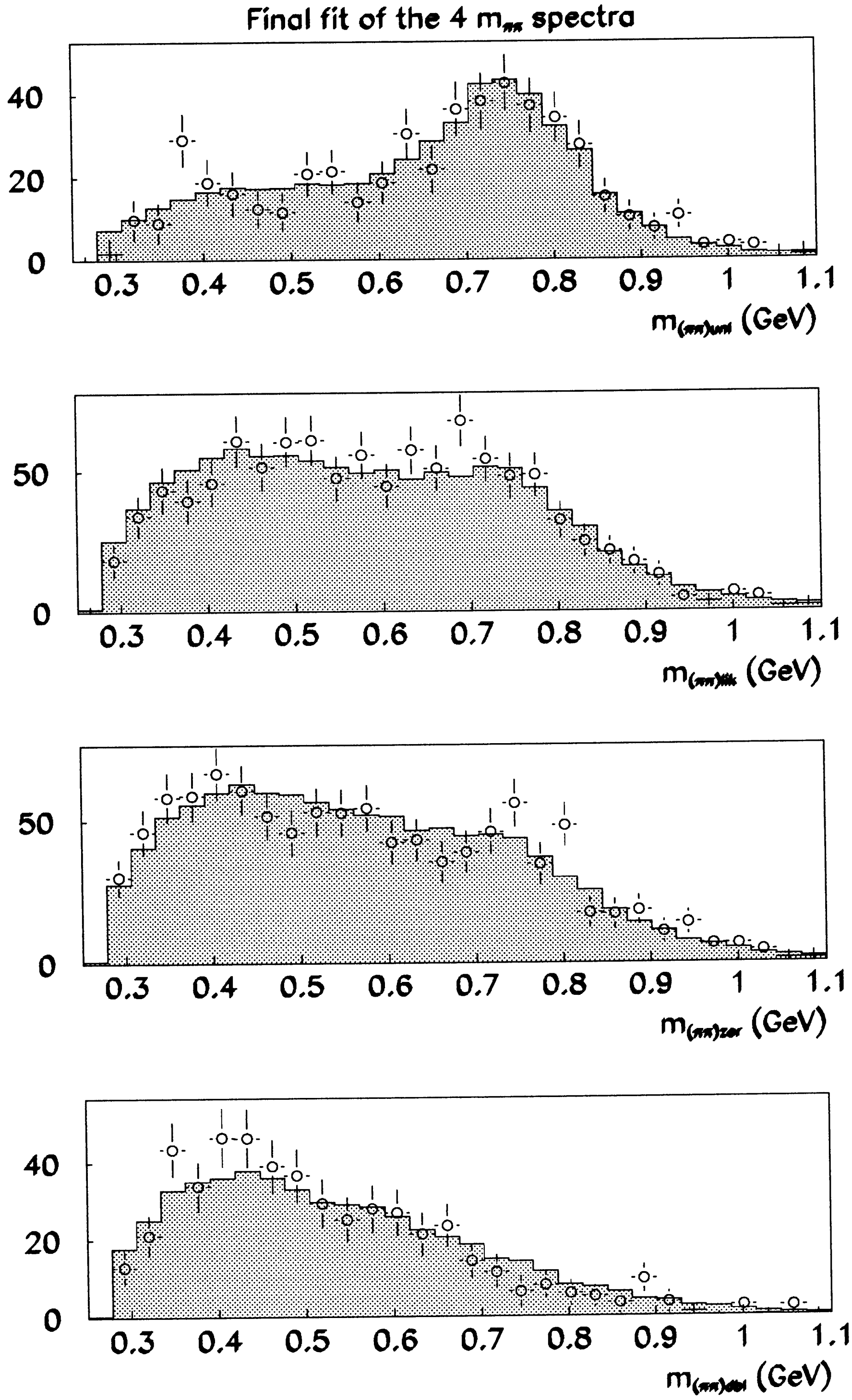

Figure 9: All possible data $m_{(\pi\pi)}$ spectra (dots) are rather well reproduced by $\Sigma = 56.2\%$ and $\Delta = 13.4\%$ (shaded)

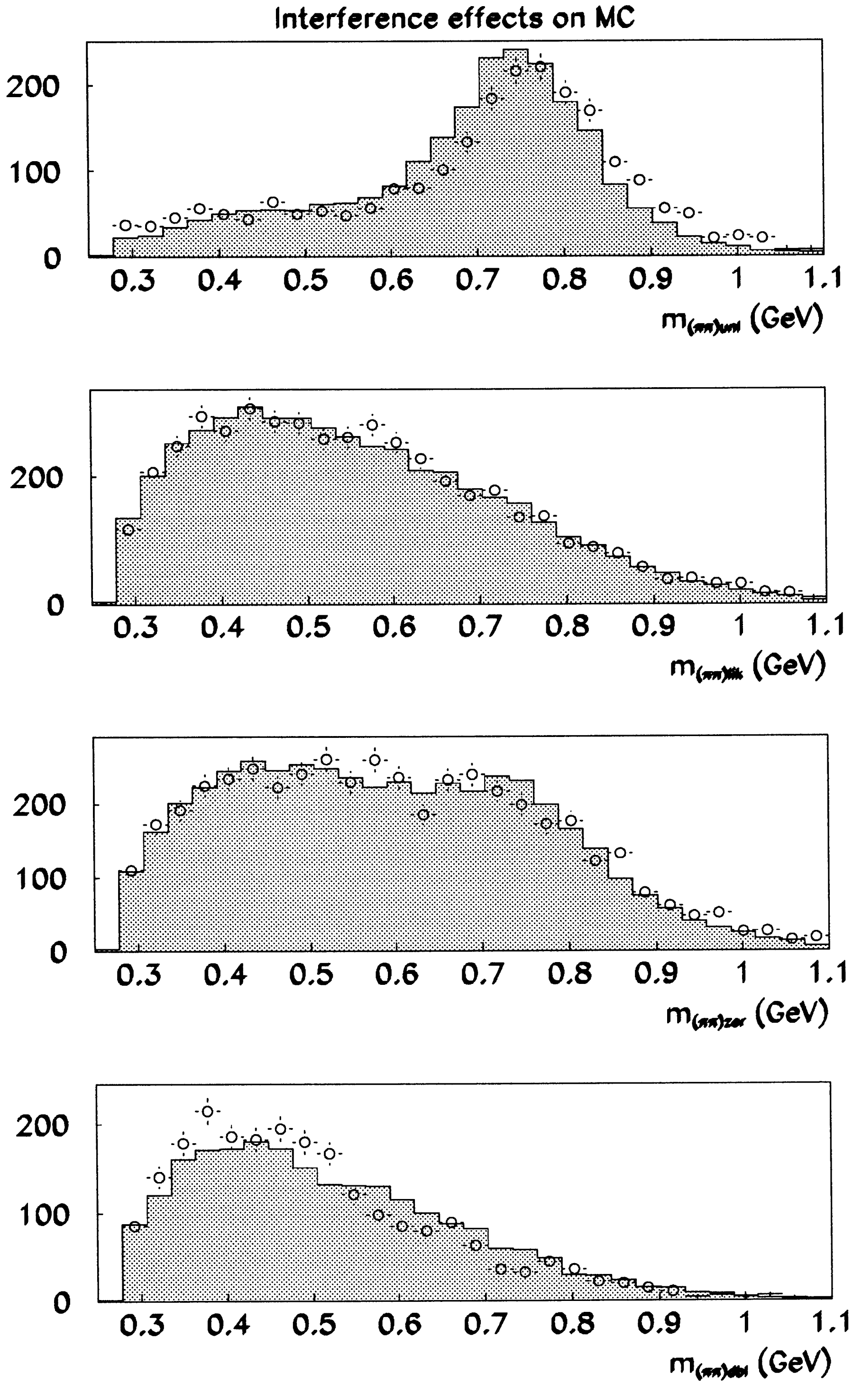

Figure 10: Performance of the fit on the Monte-Carlo. The disagreements reveal the difference between the dotted full spectrum (coherent sum) and the best fitting linear superposition (shaded histogram)

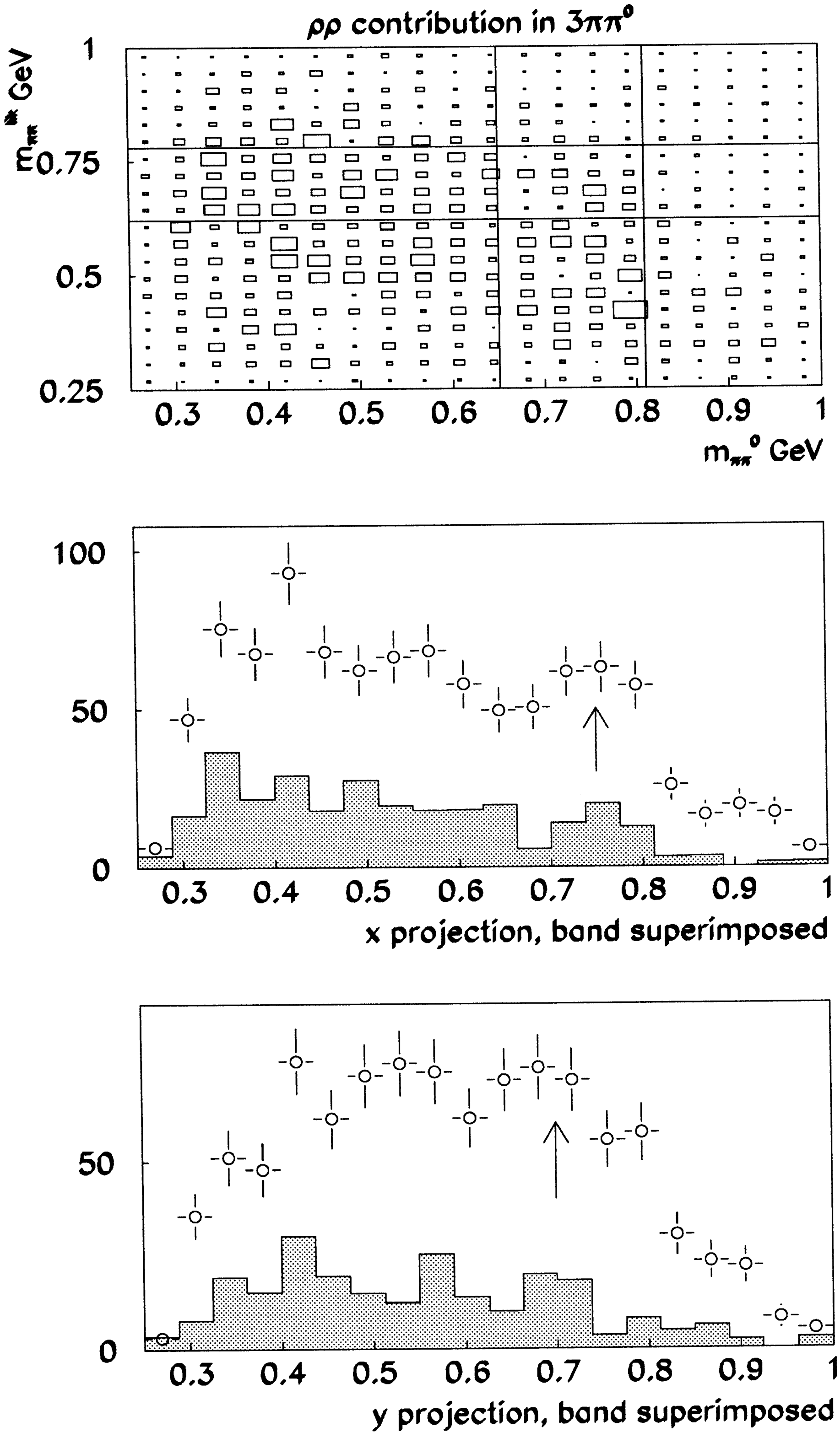

Figure 11: $m_{(\pi\pi)^{lik}}$ *vs* $m_{(\pi\pi)^0}$ above, projections on x and y axis below. The shaded histograms represent the projections of the bands drawn on the 2D-plot which localise the $(\rho - \rho)_p$ area